J. Biochem. **144,** 95–106 (2008)
doi:10.1093/jb/mvn050

Chemical and Apoptotic Properties of Hydroxy-Ceramides Containing Long-Chain Bases with Unusual Alkyl Chain Lengths

Mamoru Kyogashima[1,2,*], Keiko Tadano-Aritomi[3], Toshifumi Aoyama[4], Akiko Yusa[1], Yoshiko Goto[1], Keiko Tamiya-Koizumi[1,5], Hiromi Ito[5], Takashi Murate[5], Reiji Kannagi[1] and Atsushi Hara[4]

[1]Division of Molecular Pathology, Aichi Cancer Center Research Institute, 1-1 Kanokoden, Chikusa-ku, Nagoya, Aichi, 464-8681; [2]Department of Oncology, Graduate School of Pharmaceutical Sciences, Nagoya City University, 3-1 Tanabe-dori, Mizuho-ku, Nagoya, 467-8603; [3]Department of Biochemistry, Teikyo University School of Medicine, 2-11-1 Kaga, Itabashi-ku, Tokyo, 173-8605; [4]Department of Metabolic Regulation, Institute on Aging and Adaptation, Shinshu University Graduate School of Medicine, 3-1-1 Asahi, Matsumoto, Nagano, 390-8621; and [5]Department of Medical Technology, Nagoya University Graduate School of Health Sciences, 1-1-20, Daiko-Minami, Higashi-ku, Nagoya, Aichi, 461-8673, Japan

Received February 29, 2008; accepted March 20, 2008; published online April 16, 2008

We analysed four types of free ceramides (Cer 1, Cer 2, Cer 3 and Cer 4) from equine kidneys by electrospray ionization mass spectrometry. Cer 1 was composed of dihydroxy long-chain bases (dLCBs) of (4E)-sphingenine (d18:1), sphinganine and non-hydroxy fatty acids (NFAs); Cer 2 was composed of trihydroxy LCBs (tLCBs) of 4-hydroxysphinganine, t16:0, t18:0, t19:0 and t20:0, and NFAs; Cer 3 was composed of dLCBs, d16:1, d17:1, d18:1, d19:1 and d20:1, and hydroxy FAs (HFAs); and Cer 4 was composed of tLCBs, t16:0, t17:0, t18:0, t19:0 and t20:0, and HFAs. The results indicate all ceramide species containing LCBs with non-octadeca lengths (NOD-LCBs) can be classified into hydroxy-ceramides since these species always consist of tLCBs, and/or HFAs. Furthermore, such species tend to contain FAs with longer acyl chains but contain neither palmitate (C16:0) nor its hydroxylated form (C16:0h). The apoptosis-inducing activities of these hydroxyl-ceramides towards tumour cell lines were compared with that of non-hydroxy-ceramides, dLCB-NFA (Cer 1). Monohydroxy-ceramides, tLCB-NFA (Cer 2) and dLCB-HFA (Cer 3), exhibited stronger activities, whereas dihydroxy-ceramides, tLCB-HFA (Cer 4), exhibited similar or weaker activity than dLCB-NFA (Cer 1), depending on cell lines.

Key words: apoptosis, ceramides, hydroxy-ceramides, long-chain bases, mass spectrometry.

Abbreviations: C16:0h, C16:0 hydroxy fatty acid; d18:1-C16:0, ceramide possessing d18:1 with C16:0; dLCB, dihydroxy long-chain base; d16:1, (4E)-hexadecasphingenine; d17:1, (4E)-heptadecasphingenine; d18:0, sphinganine; d18:1, (4E)-sphingenine; d19:1, (4E)-nonadecasphingenine; d20:1, (4E)-icosasphingenine; ESI, electrospray ionization; HFA, hydroxy fatty acid; HPTLC, high performance thin-layer chromatography or chromatogram; MS, mass spectrometry; NFA, non-hydroxy fatty acid; NOD-LCBs, non-octadeca LCB; OD-LCBs; octadeca LCBs; PARP, poly ADP-ribose polymerase; 7-AAD, 7-amino-actinomycin D; tLCB; trihydroxy LCB; t16:0, 4D-hydroxyhexadecasphinganine; t17:0, 4D-hydroxyheptadecasphinganine; t18:0, 4D-hydroxysphinganine or phytosphingosine; t19:0, 4D-hydroxynonadecasphinganine; t20:0, 4D-hydroxyicosasphinganine.

Ceramide (*N*-acylated long-chain base) is a basic component of glycosphingolipids and phoshosphingolipids (*1*). Although abundant free ceramides are present in skin, and act as a water reservoir and a barrier due to their physicochemical properties (*2*), in most cells, free ceramides are bioactive and play important roles in cell signalling for differentiation, growth and apoptosis; and therefore their amounts are strictly regulated (*3–6*). Mass spectrometry (MS) using a soft ionization technique is a powerful tool to determine individual ceramide molecular species, and many reports have been published on its use (*7–11*). However, reports of ceramides containing non-octadeca long-chain bases (NOD-LCBs) such as d16:1/t16:0, d17:1/t17:0, d19:1/t19:0 in mammals are limited (*10*, *12–14*) and their functions remain unclear. Therefore, there is a need for a more detailed basic analysis of free ceramides using substantial amounts of biological materials. We previously purified four types of ceramides from equine kidneys by column chromatography, and analysed their fatty acid (FA) and LCB compositions by gas–liquid chromatography (*15*). The results indicated that Cer 1, Cer 2, Cer 3 and Cer 4 were composed of d18:1 and NFAs; 4-hydroxysphinganine (t18:0), 4-hydroxyicosasphinganine (t20:0) and NFAs; d18:1 and HFAs; and t18:0, t20:0 and HFAs; respectively; although the exact combination of LCBs and FAs was not determined. Very recently, we reported the diversity of molecular species of ceramides in rat sulphated glycosphingolipids (sulphatides) containing uncommon LCBs of sphingadienine (d18:2), (4E)-icosasphingenine (d20:1)

*To whom correspondence should be addressed. Tel: +81 52 762 6111, Fax: +81 52 763 5233, E-mail: mkyogashi@aichi-cc.jp

and icosasphinganine (d20:0), together with d18:1 and t18:0. Furthermore, we demonstrated an interesting relationship between LCBs and FAs, *i.e*. ceramides of sulphatide SM4s (HSO_3-3Galβ1Cer) were mainly d18:1 and C24:0h (C24 HFA) whereas those of SM2 (GalNAcβ4(HSO_3-3)Galβ4Glcβ1Cer) were mainly composed of t18:0 and C24:0 (C24 NFA), indicating that different series of sulphatides contain different but incidentally similar hydroxy-ceramides** with respect to carbon chain lengths of fatty acid and LCB (*16*). Therefore, we hypothesized the regulatory mechanisms controlling combinations of LCBs and FAs in the kidneys. In the present study, we analysed ceramides using electrospray ionization (ESI) MS with low-energy collision-induced dissociation, and identified various species of hydroxy-ceramides containing novel NOD-LCBs. Furthermore, we compared the apoptosis-inducing activities of hydroxy-ceramides with that of non-hydroxy-ceramides towards human tumour cell lines.

MATERIALS AND METHODS

Materials—Standard ceramides of d18:1-C16:0, d18:1-C24:0, d18:0-C18:0, d18:0-C24:0 were purchased from Avanti (Alabaster, AL, USA). Ceramides containing d18:1-24:0h and t18:0-C24:0h were prepared from kidneys of saposin $D^{-/-}$ mice (*17*). HPTLC plates (silica gel 60) were from Merck (Darmstadt, Germany). Rabbit polyclonal anti-poly ADP-ribose polymerase (PARP) and caspase-3 activity assay kit, BV-K106, were purchased from Biomol International L.P. (Plymouth Meeting, PA, USA) and MBL Co., Ltd. (Nagoya, Japan), respectively. ECL western blotting detection system was from GE Healthcare (Buckinghamshire, UK). Biotin-conjugated annexin V, binding buffer for annexin V and 7-amino-actinomycin D (7-AAD) were purchased from BD biosciences (San Jose, CA, USA). FITC-streptavidin was purchased from Zymed Laboratories (South San Francisco). All other reagents were of the highest grade commercially available in Japan.

Ceramides from Equine Kidneys—Equine kidneys were purchased from a slaughterhouse. A ceramide mixture was isolated from the kidneys, as previously described (*15*). Briefly, lipids were extracted with a chloroform-methanol mixture. The ceramide-rich fraction was obtained after solvent partition and silica gel column chromatography. Four distinct bands, detected by HPTLC of the mixture, were separated from each other by preparative HPTLC developed with chloroform: methanol: glacial acetic acid (95 : 1 : 4; v:v:v). The final isolated products are shown in Fig. 1.

MS—Characterization of each ceramide fraction was performed by negative-ion ESI-MS as previously described (*17*) using an LCQ DECA ion trap mass spectrometer fitted with an ESI ion source (inner diameter = 0.1 mm) (Thermo Fisher Scientific Inc, San Jose, CA, USA). Approximately 10–20 μg/ml ceramides in absolute methanol were directly infused into the ion source at a flow rate of 3 μl/min. Molecular-related ions were detected as $[M–H]^-$ ions. The heated capillary was set at 250°C, and spray voltage was set at 5 kV. Sheath gas flow rate was set to 50 in arbitrary units. Low-energy collision-induced dissociation was carried out on the molecular-related ion (MS^2) using helium gas present in the ion trap. The relative collision energy used ranged from 30% to 40%.

Fig. 1. **HPTLC of purified ceramides from equine kidneys.** The plate was developed with chloroform:methanol : glacial acetic acid (95 : 1 : 4; v:v:v), and visualized by spraying cupric phosphoric acid, and charring at 180°C for 15 min. The double bands in Cer 1 reflected the difference of FA chain lengths because the upper band co-migrated with chemically synthesized authentic d18:1-C24:0 and the lower band co-migrated with that of d18:1-C16:0 (data not shown).

Cytotoxic Activities of Ceramides—The cytotoxic activities of four different ceramides were examined using a human neuroblastoma cell line, SH-SY5Y, and leukaemia cell lines, K562 and HL60. SH-SY5Y cells were cultured in 10% FCS in DMEM, while leukaemia cell lines were cultured in 10% FCS in RPMI1640. Addition of ceramides to culture media was according to Ji *et al*. (*18*). Briefly, ceramides were first dissolved in a solvent mixture of ethanol/dodecane, (98:2, v:v) and added to media to adjust the final concentrations of each ceramide to be at 0.1 to 10 μM and the final ethanol concentration to be <0.1%. The viable cells were counted by a trypan blue dye exclusion method in triplicate. Viable cell number (%) was defined here as the percentage of viable cells to the initial seeding cell concentration.

Flow Cytometry—Apoptosis was confirmed as exposure of phosphatidylserine on cell surface (*19*). After cells were cultured with or without the respective ceramides for 16 h, they were harvested and incubated with or without biotin-conjugated annexin V for 20 min on ice. After being washed with the binding buffer, the cells were incubated with a 1 : 100 dilution of FITC-streptavidin for 20 min on ice. The cells were washed and incubated with a 1 : 200 dilution of 7-AAD. The cells were evaluated by flow cytometry with FACSCalibur (Becton Dickinson, Mountain View, CA, USA).

Determination of Caspase-3 Activity—Activation of caspase-3 induced by ceramides was determined. HL 60 cells were treated with or without 0.2 μM of ceramides. After 16 h, the cells were collected and protein was determined with Bradford reagent using bovine serum

** Hydroxy-ceramides are defined hereinafter as ceramides that contain a trihydroxy long-chain base (tLCB), an hydroxy fatty acid (HFA), or both.

albumin as the standard. Cell lysates of 5 μg protein equivalent were analysed by western blot using the anti-PARP antibody. Simultaneously, the caspase-3 activity was measured in triplicate using 50 μg protein of cell lysates as the enzyme source and DEVD-*p*NA as a synthetic substrate, according to the manufacture's protocol.

Statistics—Student *t*-tests were used to compare the values obtained between the two groups. A *P*-value of <0.05 was considered to be statistically significant.

RESULTS

Full-Scan Spectra of Cer 1, Cer 2, Cer 3 and Cer 4 by Negative Ion ESI-MS—Former analyses using gas–liquid chromatography showed that Cer 1, Cer 2, Cer 3 and Cer 4 were mainly composed of d18:1 with NFA, t18:0 with NFA, d18:1 with HFA and t18:0 with HFA, respectively (*15*). Figure 2A–D shows full-scan spectra of Cer 1, Cer 2, Cer 3 and Cer 4, respectively, where only $[M–H]^-$ ions, without Cl adduct, were observed as molecular related ions. Two similar patterns in terms of distribution of molecular related ion abundance were found : one for Cer 1 and Cer 3, and another for Cer 2 and Cer 4. Eighteen molecular mass difference between 648 in Cer 1 and 666 in Cer 2, suggested occurrences of d18:1-C24:0 at 648 in Cer 1 and t18:0-24:0 at 666 in Cer 2. Likewise, 16 and 34 molecular mass differences between 648 in Cer 1 and 664 in Cer 3, and 648 in Cer 1 and 682 in Cer 4 suggested occurrences of d18:1-C24:0h at 664 in Cer 3 and t18:0-C24:0h at 682 in Cer 4, respectively. These relationships were consistent with former analytical results.

Product Ion (MS^2) Spectra of $[M–H]^-$ Ions of Cer 1 and Cer 3—Figure 3A shows fragmentation schemes of Cer 1 and Cer 3. Figure 4A shows the product ion spectrum of 634 in Cer 1. As previously reported, ions from the common structure of ceramides at 616 [M–H–H_2O], 604 [M–H–H_2CO], 602 [M–H–H_2–H_2CO] and 586 [M–H –H_2O–H_2CO]; a series of ions from FAs at 394 (a3–H_2), 378 (a3–H_2O) and 352 (a2); and an ion at 298 (b2) derived from LCB d18:1 were observed (*9*). Figure 4B shows the product ion spectrum of m/z 552 in Cer 3, which, like other components of that band, represents characteristic reporter ions of ceramide containing HFA, a3 related ions. As previously reported, a series of ions from a FA, 271 (a2′), 296 (a3–H_2O) and 312(a3–H_2) were observed in addition to ions from the common structure of ceramides at 534 [M–H–H_2O], 516 [M–H–$2H_2O$] and 504 [M–H–H_2O–H_2CO]. These product ions together with an ion at 298 derived from the LCB of d18:1 (*9*), confirmed that an ion at 552 in Cer 3 corresponded to the $[M–H]^-$ ion of d18:1-C16:0h. Accordingly, the ion at 622 was expected to be the $[M–H]^-$ ion of d18:1-C21:0h. However, surprisingly, MS^2 of the $[M–H]^-$ ion at 622 in Cer 3 produced several unexpected ions together with the ions from the common structure of ceramides at 604, 586 and 574 (Fig. 4C and D). In addition to a series of ions derived from C21:0h, 341/366/382, two additional series of ions, *i.e.* at 355/380/396 and 369/394/410, were observed (Fig. 4D), where the difference between 355/380/396 and 369/394/410 (14 Da) corresponded to a ($-CH_2-$) unit. Besides, product ions derived from the LCB were observed at 284, 270 and 298; and the signal at 298 corresponded to d18:1 (Fig. 4D); indicating that the ion at 622 in Cer 3 was composed of three species of ceramides, *i.e.* d18:1-C21:0h, d17:1-C22:0h and d16:1-C23:0h. Furthermore, judging from peak heights, d16:1-C23:0h was the most abundant and d17:1-C22:0h was also present in a significant amount. Table 1 summarizes the detected ions in product ion spectra of Cer 1 and Cer 3. The ceramide species with common dLCBs such as d18:1 or d18:0 contained NFAs/HFAs with acyl chain lengths of C16 to C26, whereas those with non-octadeca dLCBs such as d16:1, d17:1, d19:1 and d20:1 tended to contain NFAs/HFAs with longer acyl chains but contained neither palmitate (C16:0) nor its hydroxylated form (C16:0h).

Product Ion (MS^2) Spectra of $[M–H]^-$ Ions of Cer 2 and Cer 4—Figure 3B shows fragmentation schemes of Cer 2 and Cer 4, which contain tLCBs. Figure 5A shows the product ion spectrum of 666 in Cer 2. As previously reported, ions from the common structures of ceramides at 648 [M–H–H_2O], 634 [M−H–H_2–H_2CO] and 630 [M–H–$2H_2O$]; ions from FA at 367 (a2′), 410 (a3) and 422 (a4–H_2O); ions from the LCB t18:0 at 267 [b2–(CH_2OH)–H_2O] and the less abundant ion at 284 [b2–(CH_2OH)–H], were observed (*9*), indicating that the ion at 666 corresponded to the $[M–H]^-$ ion of t18:0-C24:0. In addition, by careful observation, less abundant ions at 382 (a3), 394 (a4–H_2O) and 295 [b2–(CH_2OH)–H_2O] were recognized, indicating the co-existence of small amounts of $[M–H]^-$ ions derived from t20:0-C22:0 in 666. Interestingly, a series of ions at 367 (a2′), 410 (a3) and 422 (a4–H_2O) were observed once again, in the product ion spectrum of 694 (Fig. 5B), and ions from the major LCB were not 267/284 but 295/312, indicating that the predominant $[M–H]^-$ ion for 694 was from t20:0-C24:0. Furthermore, less abundant ions at 395 (a2′), 438 (a3), 450 (a4–H_2O) and 267 indicated that small amounts of t18:0-C26:0 were also included in 694.

We previously reported that in the product ion spectrum of t18:0-C24:0h [$M–H^-$, 682], ions from the FA moiety were composed of an abundant ion at 383 (a2′) and less abundant ions at 426 (a3) and 438 (a4–H_2O). Accordingly, if the $[M–H]^-$ ion at 696 in Cer 4 consists of a single ceramide species of t18:0-C25:0h, ions from FAs should be detected at 397 (a2′), 440 (a3) and 452 (a4–H_2O). In the present study, two additional groups of ions, *i.e.* 383/426/438 and 369/412/424 were observed in the MS^2 spectrum of Cer 4 (Fig. 5C). Correspondingly, three groups of ions from LCBs were observed in 696 at 267/284, 281/298 and 295/312 (Fig. 5C and D). These results clearly indicated that the ion at 696 was composed of the most abundant species of t20:0-C23:0h together with the less abundant species of t18:0-C25:0h and t19:0-C24:0h. Table 2 summarizes the detected ions in product ion spectra of Cer 2 and Cer 4. Most deprotonated molecules of Cer 2 and Cer 4 are composed of more than two species of ceramides, and this trend is more obvious in Cer 4. However, it should be noted that $[M–H]^-$ ions at 554 in Cer 2 and 570 in Cer 4 are composed of single molecular species of t18:0-C16:0 and t18:0-C16:0h, respectively.

Apoptosis Induced by the Ceramides on Tumour Cells—Cytotoxic activity induced by ceramides on HL60,

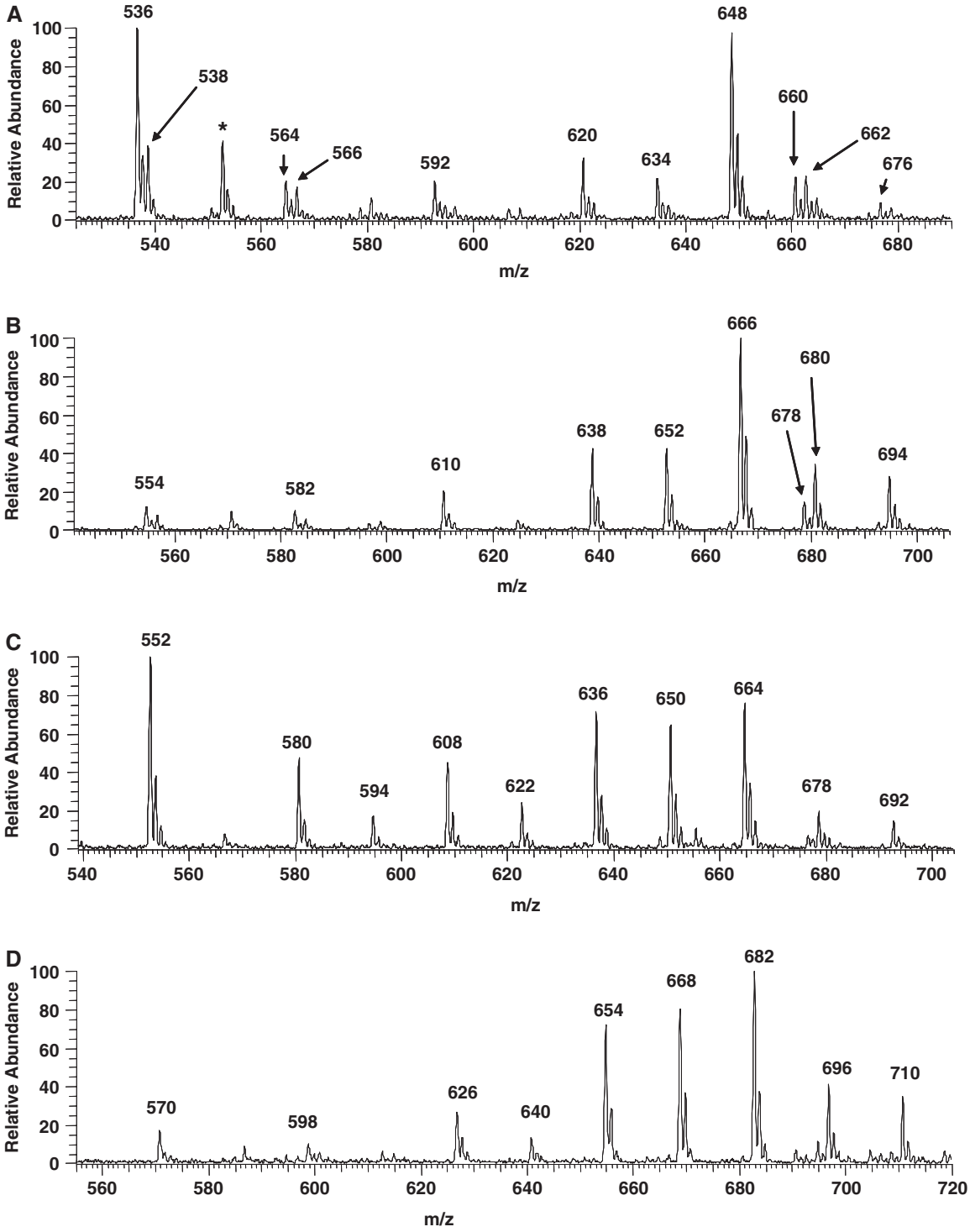

Fig. 2. **Full-scan spectra of purified ceramides from equine kidneys by ESI-MS.** (A) Cer 1, (B) Cer 2, (C) Cer 3 and (D) Cer 4. Asterisk implies not analysed (see text).

K562 and SH-SY5Y were shown in Fig. 6A–C, respectively. While all types of ceramides induced cell death at <1 μM in HL60 cells, ~10 times higher concentrations were required for K562 and SH-SY5Y cells. In order to confirm whether the cell death induced by hydroxylceramides was due to apoptosis, phosphatidylserine on their cell surface were detected by flow cytometry (Fig. 7A) (*19*). Although concentrations of ceramides for induction of apoptosis are dependent on tumour cell types, there are consistent relationships between ceramide species and their apoptosis-inducing-activities. Monohydroxyceramides (Cer 2 and Cer 3), especially Cer 3, exhibited

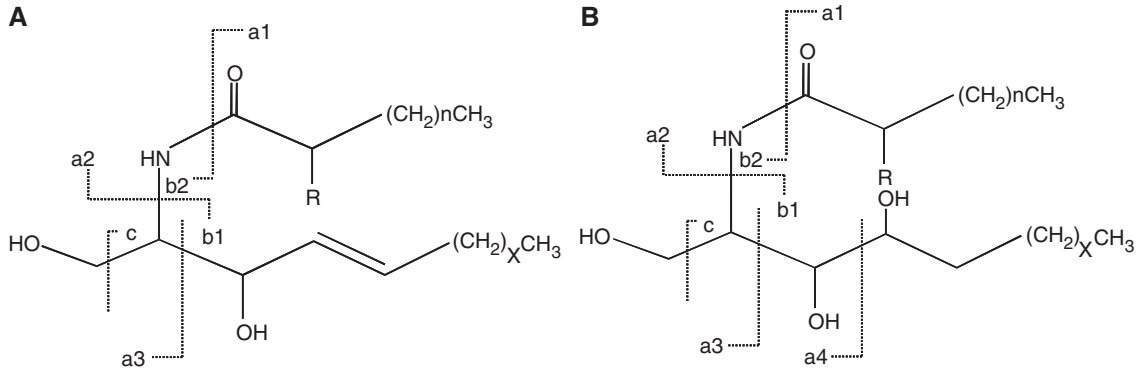

Fig. 3. **Fragmentation scheme of ceramides by ESI-MS^2.** Ion designations: species denoted with 'a' are FA-related; species denoted with 'b' are LCB-related ions, and species denoted with 'c' are common ions. $n = 13–23$, $X = 10–14$. (A) Ceramides possessing dLCBs. Cer 1 (R = H), Cer 3 (R = OH); (B) Ceramides possessing tLCBs. Cer 3 (R = H), Cer 4 (R = OH), (modified from ref. *16*). dLCBs except d18 : 0 have alkenyl chains and no tLCBs have alkenyl chains in equine kidney.

stronger activities, whereas dihydroxy-ceramide (Cer 4) exhibited similar or rather weaker activity as compared with non-hydroxy-ceramide (Cer 1) (Fig. 6). For further confirmation, we analysed caspase-3 activity using HL60 cells. As shown in Fig. 7B, the fragmented PARP (85 kDa) cleaved by caspase-3 (*20*) was detected by western blot after the cells were treated with 0.2 μM of Cer 2 and Cer 3 for 16 h. It should be noted that the intensity of fragmented 85 kDa band in Cer 3 was stronger than that in Cer 2. Elongation of incubation period or increase of the concentration of Cer 1 and Cer 4 could induce fragmented PARP in the cells (data not shown). Caspase-3 activities in the cells were directly measured using a synthetic substrate. As in Fig. 7C, caspase 3 activity was induced most strongly by Cer 3, followed by Cer 2. It was induced only weakly by Cer 1 and Cer 4. These results are very consistent with those in Fig. 6A.

DISCUSSION

We analysed four purified ceramides from equine kidneys by ESI-MS, in the negative ion mode. Low-energy CID with the selection of the $[M–H]^-$ ion as the precursor revealed an unexpected complexity of ceramide species. In addition to OD-LCBs such as d18:1, d18:0 and t18:0, we identified ceramides containing NOD-LCBs such as d16:1, d17:1, d19:1, d20:1, t16:0, t17:0, t19:0 and t20:0. These results instructively notify us to consider possible occurrence of NOD-LCBs on analysis of sphingolipids, especially using MS. In this experiment, we adopted ESI-MS method, which facilitated us to analyse these unexpected complexities.

Ceramides with d18:1 such as Cer 1 and Cer 3 contained a broad-length range of fatty acyl chains from C16 to C26, either non-hydroxylated or hydroxylated. Ceramides containing d18:1 with NFAs are *de novo* synthesized through several steps. Firstly, serine palmitoyltranferase catalyzes condensations of L-serine and palmitoyl-CoA to produce 3-ketosphinganine, which is then reduced to d18:0 by 3-ketosphinganine reductase (*21–24*). Dihydroceramide synthases *N*-acylate d18:0 to produce dihydroceramides (*25*). Recently, LASS genes encoding for dihydroceramide synthases were reported to be comprised of six members in mammals; interestingly, each LASS protein preferentially transfers specific lengths of acyl chains (*26–29*). LASS 2, 5 and 6 are reported to be expressed in kidneys and LASS 2 transfers C24:0 whereas LASS 5 transfers C18:0, C20:0 and C24:0, and LASS 6 transfers C16:0 (*29*). Accordingly, we suggest that these LASS proteins in equine kidney may synthesize ceramides found in Cer 1, although the transfer of odd numbers of fatty acyl chains has not been reported. Finally, the equine dihydroceramide desaturase, DES 1 (*30*) and maybe DES2 proteins (*31*) could probably convert these d18:0-NFAs to d18:1-NFAs.

On the other hand, the synthetic pathway of ceramides containing d18:1 with HFA remains unclear. FA2H was reported as a mammalian fatty acid 2-hydroxylase (fatty acid α-hydroxylase), which could directly hydroxylate free FAs with various acyl chain lengths of C16:0 to C26:0 (*32*, *33*). However, to the best of our knowledge, there has been no report whether the LASS protein known as (dihydro)ceramide synthase (*26–29*) could transfer HFA to d18:0. If this was the case, it is unclear which LASS protein can transfer specific HFAs. In addition, it has not been clarified whether DES 1 protein could convert d18:0-HFA to d18:1-HFA. A different possible pathway has also been suggested, *i.e.* FA2H hydroxylates fatty acyl chains of d18:1-NFAs to d18:1-HFAs (*34*). Profiles of full-scan spectra for Cer 1 and Cer 3 appeared similar to those for Cer 2 and Cer 4, suggesting close metabolic relationships between Cer 1/Cer 3, and Cer 2/Cer 4 (Fig. 2). On the other hand, although they were similar, profiles of Cer 1 and Cer 3 were slightly different. In Cer 1, ions at 536 (d18:1-C16:0) and 648 (d18:1-C24:0) were dominant, whereas in Cer 3, in addition to the corresponding ions at 552 (d18:1-C16:0h) and 664 (mainly d18:1-C24:0h), other ions at 608 (mainly d18:1-C20:0h), 636 (mainly d18:1-C22:0) and 650 (mainly d18:1-C23:0) were also prominent. This pattern may be partly due to the co-existence of other isomeric ceramide species, suggesting that there are some enzymatic preferences in the hydroxylation step for the synthesis of d18:1-HFAs.

The full-scan spectrum of Cer 1 was very different from that of Cer 2 with respect to intensities of ions containing C16 NFA (536 of Cer 1 and 554 of Cer 2). The species in Cer 2, whose major LCB was t18:0, were probably converted

from d18:0-NFAs by a bifunctional enzyme of DES2 protein (*30*, *31*, *35–37*). The difference in intensity of 536/554 suggests that DES 2 may prefer ceramide species with longer FAs as substrates, although such a preference has not been reported. No enzyme has been reported to directly hydroxylate d18:0 to t18:0 in mammals, although such an enzyme was found in fungi (*38*).

The relationship between Cer 1 and Cer 3 was similarly observed between Cer 2 and Cer 4. Careful examination of full-scan spectra showed that ions at 666 (mainly t18:0-C24:0) were dominant in Cer 2, whereas in Cer 4 other ions, such as at 654 (mainly t18:0-C22:0h) and 668 (mainly t18:0-C23:0h), were also prominent as well as at 682 (mainly t18:0-C24:0h). Ceramides of t18:0-HFAs might be synthesized from d18:0-HFAs by DES 2, or from t18:0-NFA by FA2H.

The proposed *de novo* synthetic pathway for ceramides possessing OD-LCBs is summarized in Fig. 8. In addition, dihydroceramide synthase was reported to transfer NFAs not only to d18:0, but also to d18:1 and t18:0 (*25*),

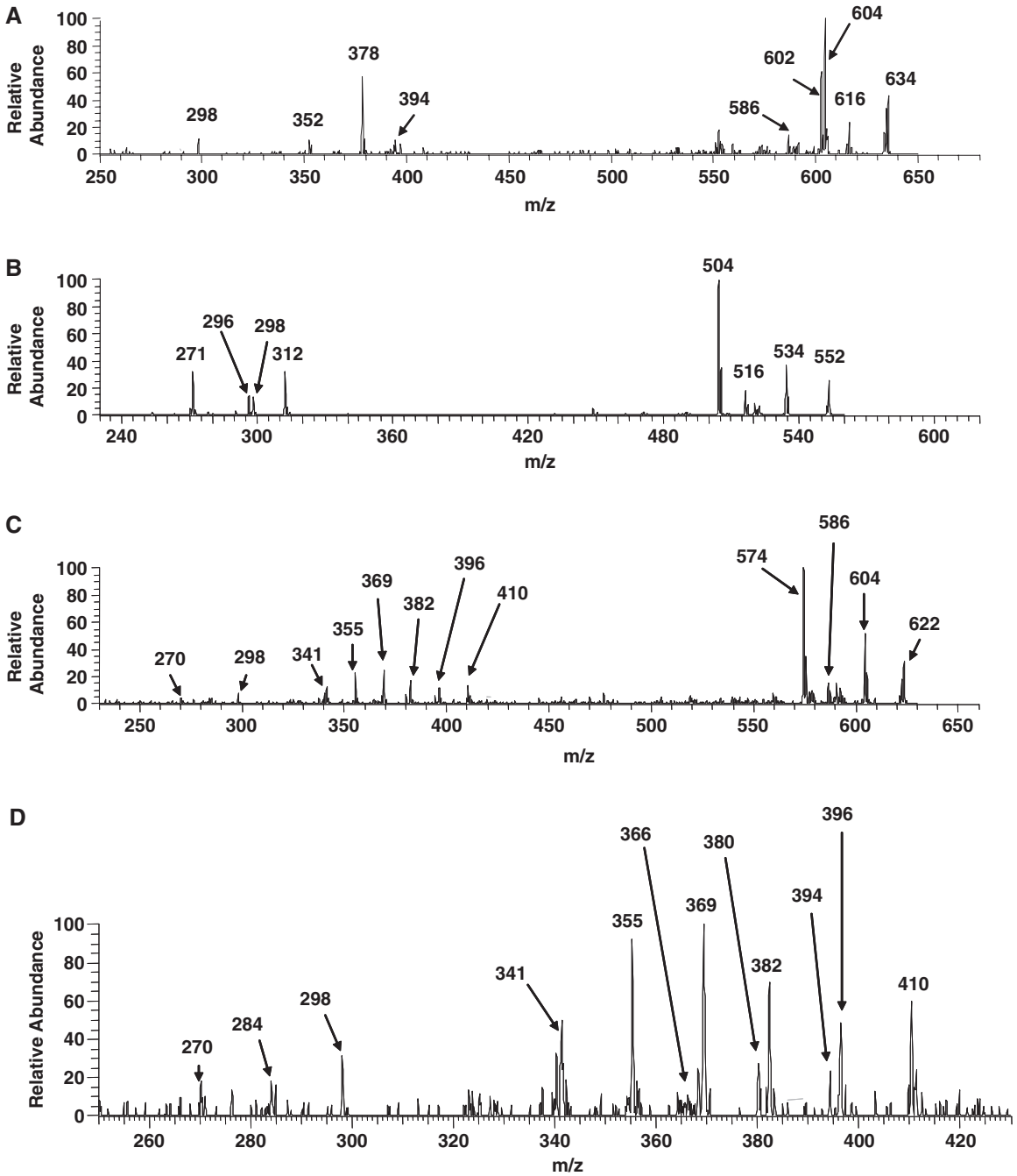

Fig. 4. **Product ion spectra of Cer 1 and Cer 3 by ESI-MS^2.** The [M–H]$^-$ ion selected as the precursor was 634 in Cer 1 (A); 552 in Cer 3 (B); 622 in Cer 3 (C). (D) Enlarged spectrum of (C).

Table 1. **Identified ions in Cer 1 and Cer 3 by ESI-MS^2.**

Cer 1	$[M–H]^-$	$m–H_2O$	$m–H_2CO$	$m–H_2–H_2CO$	$m–2H_2O$	$m–H_2O–H_2CO$	a2	a2′	$a3–H_20$	$a3–H_2$	a3	b2
d18:1-C16:0	536	518	506	504		488	254	255	280	296	298	298
d18:0-C16:0	538	520	508	506		490	254	255	280	296	298	300
d18:1-C18:0	564	546	534	532		516	282	283	308	324	326	298
d18:0-C18:0	566	548	536	534		518			308	324	326	300
d18:1-C20:0	592	574	562	560		544	310	311	336	352		298
d18:1-C22:0	620	602	590	588		572	338	339	364	380		298
d18:1-C23:0	634	616	604	602		586	352	353	378	394	396	298
d18:1-C24:0	648	630	618	616		600	366		392	408		298
d18:1-C25:1	660	642	630	628		612	378		404			300
d18:1-C25:0	662	644	632	630		614	380	381	406	422	424	298
d18:1-C26:0	676	658	646	644		628	394	395	420	436		298
Cer 3	$[M–H]^-$	$m–H_2O$	$m–H_2CO$	$m–H_2–H_2CO$	$m–2H_2O$	$m–H_2O–H_2CO$	a2	a2′	$a3–H_20$	$a3–H_2$	a3	b2
d18:1-C16:0h	552	534			516	504		271	296	312		298
d16:1-C20:0h[a]	580	562			544	532		327	352	368		270
d18:1-C18:0h	580	562			544	532		299	324	340		298
d16:1-C21:0h[a]	594	576			558	546		341	366	382		270
d17:1-C20:0h[a]	594	576			558	546		327	352	368		284
d18:1-C19:0h	594	576			558	546		313	338	354		298
d16:1-C22:0h	608	590			572	560		355	380	396		270
d18:1-C20:0h[a]	608	590			572	560		327	352	368		298
d16:1-C23:0h[a]	622	604			586	574		369	394	410		270
d17:1-C22:0h[a]	622	604			586	574		355	380	396		284
d18:1-C21:0h	622	604			586	574		341	366	382		298
d17:1-C23:0h	636	618			600	588		369	394	410		284
d18:1-C22:0h[a]	636	618			600	588		355	380	396		298
d17:1-C24:0h	650	632			614	602		383	408	424		284
d18:1-C23:0h[a]	650	632			614	602		369	394	410		298
d18:1-C24:0h[a]	664	646			628	616		383	408	424		298
d20:1-C22:0h	664	646			628	616		355	380	396		326
d18:1-C25:0h	678	660			642	630		397	422	438		298
d19:1-C24:0h	678	660			642	630		383	408	424		312
d20:1-C23:0h[a]	678	660			642	630		369	394	410		326
d18:1-C26:0h	692	674			656	644		410		452		298
d20:1-C24:0h[a]	692	674			656	644		383	408	424		326

Refer to Fig. 3 for a2, a3 and b2. m = $[M–H]^-$. a2 and a2′ are derived from $RCOO^-$ and $RCONH^-$, respectively [Hsu and Turk, (*9*)].
[a]major components in the isomer.

which might come from degradations of sphingomyelin and glycosphingolipids; this should also be considered.

Mammalian serine palmitoyltransferase has been reported to use palmitoyl-CoA as the best substrate, pentadecanoyl-/heptadecanoyl-CoA as some effective substrates and other acyl-CoAs as far less effective substrates, respectively (*21*, *23*, *24*). Actually, stearoyl-CoA and other fatty acyl-CoAs have been described in parallel to palmitoyl-CoA in SphinGOMAP (http://www.sphingomap.org) but details of the synthetic pathways for NOD-LCBs and the ceramides containing them are still uncertain. Our findings may provide clues to clarify the pathways. A regulatory system may exist in the synthetic pathways of these ceramides. Ceramide species with NOD-LCBs contained tLCBs, and/or HFAs. Such species also tended to contain FAs with longer acyl chains but contained neither palmitate (C16:0) nor its hydroxylated form (C16:0h). These results suggest that intermediate products of these ceramides may be good substrates for hydroxylases. In ceramides with NOD-LCBs, d16:1 and d17:1 are more frequently observed than those t16:0 and t17:0, whereas, t19:0 and t20:0 are more frequently observed than d19:1 and d20:1 (Table 3). Another characteristic of FAs in equine kidney ceramides is the poor amount of FA with an alkenyl chain such as nervonic acid (C24:1) which is a major component of NFA of sphingomyelin in nervous system (*39*).

It was reported that phytoceramides, kinds of monohydroxy-ceramides possessing t18:0 with NFAs, more strongly induce apoptosis in tumour cells than usual ceramides possessing d18:1-NFAs (*40*, *41*). This is consistent with our present findings that Cer 2 more strongly induced apoptosis than Cer 1. However, little is known about the apoptosis-inducing activities of monohydroxy-ceramides like dLCB-HFA (Cer 3) and dihydroxy-ceramides like tLCB-HFA (Cer 4). We found that apoptosis is induced most strongly by Cer 3, followed by Cer 2, whereas it is induced weakly by Cer 1 and Cer 4, in various human tumour cell lines. These results suggested that single hydroxylation of ceramides, especially hydroxylation at FAs, enhance apoptosis-inducing activity but double hydroxylations of ceramides both

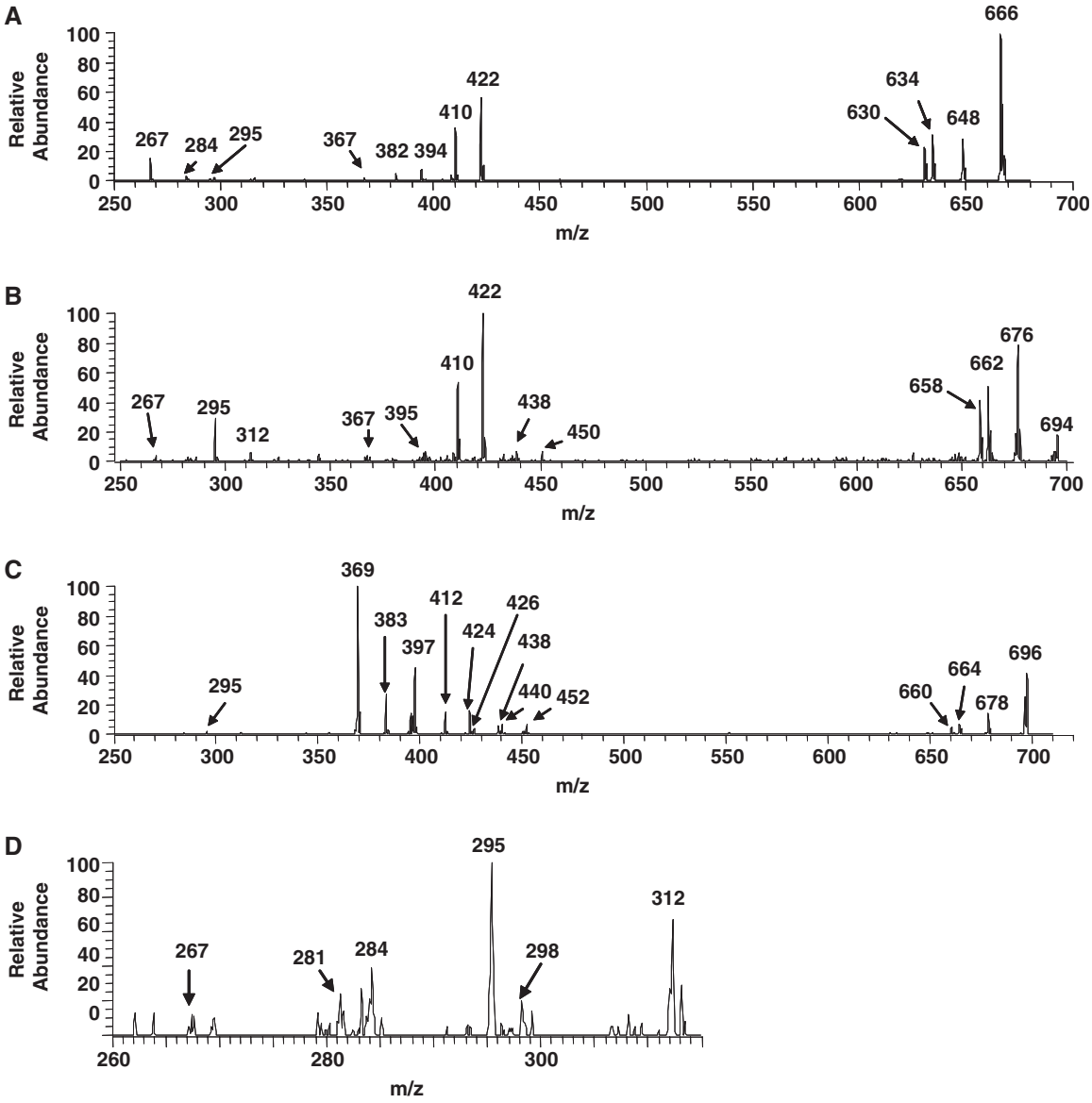

Fig. 5. **Product ion spectra of Cer 2 and Cer 4 by ESI-MS^2.** The $[M–H]^-$ ion selected as the precursor was 666 in Cer 2 (A); 694 in Cer 2 (B); and 696 in Cer 4 (C). (D) Enlarged spectrum of (C).

at LCBs and at FAs attenuated the activity. It is well known that ceramides regulate cell growth, death and differentiation by strictly controlling their amount (*3–6*). Our findings not only revealed that hydroxylations of ceramides importantly modulate cell fate, but also provided valuable information to generate more potent ceramide-based anti-cancer drugs. Since two types of monohydroxy-ceramides in the present study are still mixtures of various molecular species, determinations of the most effective and ineffective structures for inducing apoptosis remain to be investigated.

Lengths of the alkyl chain and hydroxy groups in ceramides significantly influence the physicochemical properties of sphingolipids, probably critically affecting the formation of microdomains and cell signalling (*3*, *42*). Especially, dihydroxy-ceramides are expected to create strong hydrogen bonds to neighbouring molecules. Since the ceramide moiety of sphingomyelin is generally composed of the ordinary d18:1 and NFAs, with some exceptions (*43–45*), various types of hydroxyl-ceramides including the NOD-LCBs occur as free forms, and some of them may be utilized for glycosphingolipids. Free ceramides are found not only in the plasma membrane, but also in the cell nucleus (*46*) and mitochondria (*47*, *48*) where ceramide-possessing HFAs are also reported (*47*). Various roles and the metabolic pathway of ceramides, especially hydroxy-ceramides, remain to be investigated.

This work was supported in part by a grant from NIBIO (National Institute of Biomedical Innovation).

Table 2. **Identified ions in Cer 2 and Cer 4 by ESI–MS^2.**

Cer2	$[M–H]^-$	$m–H_2O$	$m–H_2–H_2CO$	$m–2H_2O$	a2	a2′	$a3–H_2$	a3	$a4–H_2O$	$b2–(CH_2OH)–H$	$b2–(CH_2OH)–H_2O$
t18:0-C16:0	554	536	522	518		255	296	298	310	284	267
t16:0-C20:0	582	564	550	546				354	366		239
t18:0-C18:0[a]	582	564	550	546		283	324	326	338		
t18:0-C20:0[a]	610	592	578	574		311	352	354	366	284	267
t20:0-C18:0	610	592	578	574				326	338		295
t18:0-C22:0	638	620	606	602		339		382	394	284	267
t18:0-C23:0	652	634	620	616		353	394	396	408	284	267
t18:0-C24:0[a]	666	648	634	630		367	408	410	422	284	267
t20:0-C22:0	666	648	634	630		339		382	394		295
t18:0-C25:1	678	660	646	642	378	379		422	434		267
t18:0-C25:0[a]	680	662	648	644	380	381	422	424	436	284	267
t19:0-C24:0	680	662	648	644				410	422		281
t20:0-C23:0[a]	680	662	648	644		353	394	396	408	312	295
t18:0-C26:0	694	676	662	658	394	395		438	450	284	267
t20:0-C24:0[a]	694	676	662	658	366	367		410	422	312	295
Cer4	**$[M–H]^-$**	**$m–H_2O$**	**$m–H_2–H_2CO$**	**$m–2H_2O$**	**a2**	**a2′**	**$a3–H_2$**	**a3**	**$a4–H_2O$**	**$b2–(CH_2OH)–H$**	**$b2–(CH_2OH)–H_2O$**
t18:0-C16:0h	570	552	538	534		271		314	326	284	267
t16:0-C20:0h	598	580	566	564		327		370	382		
t18:0-C18:0h[a]	598	580	566	564		299		342	354	284	267
t18:0-C20:0h[a]	626	608	594	590		327		370	382	284	267
t20:0-C18:0h	626	608	594	590		299			354		
t16:0-C23:0h	640	622	608	604		369		412	424		
t17:0-C22:0h	640	622	608	604		355		398	410	270	253
t18:0-C21:0h[a]	640	622	608	604		341		384	396	284	267
t18:0-C22:0h[a]	654	636	622	618		355		398	410	284	267
t20:0-C20:0h	654	636	622	618		327		370	382		
t17:0-C24:0h	668	650	636	632		383					
t18:0-C23:0h[a]	668	650	636	632		369		412	424	284	267
t19:0-C22:0h	668	650	636	632		355		398	410		
t18:0-C24:0h[a]	682	664	650	646		383		426	438	284	267
t19:0-C23:0h	682	664	650	646		369		412	424		
t20:0-C22:0h	682	664	650	646		355		398	410		
t18:0-C25:0h	696	678	664	660		397		440	452	284	267
t19:0-C24:0h	696	678	664	660		383		426	438	298	281
t20:0-C23:0h[a]	696	678	664	660	368	369		412	424	312	295
t18:0-C26:0h	710	692	678	674		411		454	466	284	267
t20:0-C24:0h[a]	710	692	678	674		383		426	438	312	295

Refer to Fig. 3 for a2, a3 and b2. m = $[M–H]^-$. a2 and a2′ are derived from RCOO− and RCONH−, respectively. [a]Major components in the isomer.

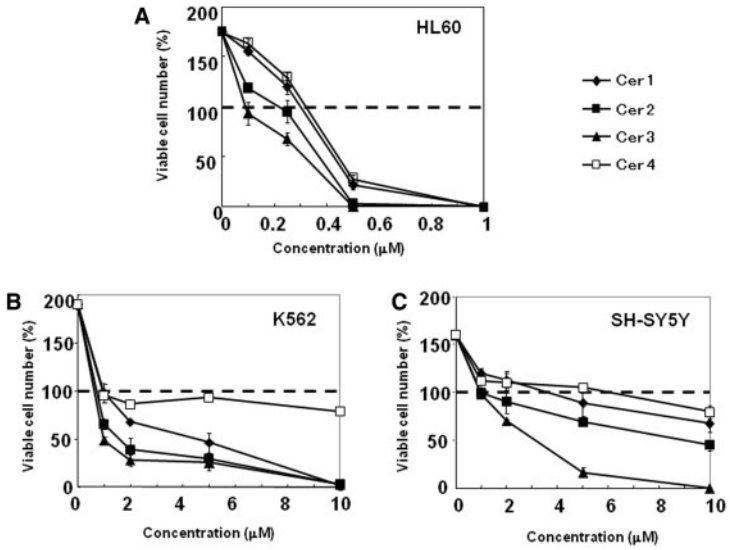

Fig. 6. **Comparison of cytotoxic activities induced by the ceramides on different human tumour cell lines, HL60 (A), K562 (B) and SH-SY5Y (C).** The viable cells were counted in triplicate by trypan blue dye exclusion after cultured with various concentrations of ceramides for 24 h. The percentage of viable cell number (%) was defined here as the percentage of viable cells to the initial seeding cells, *i.e.* if the cells were alive without proliferation, it was calculated as 100% (dotted line).

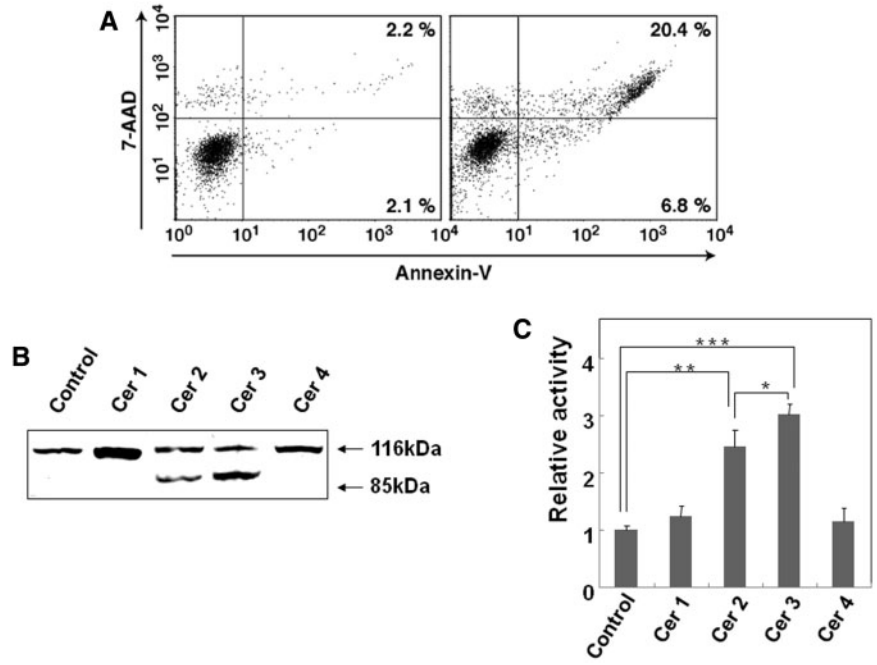

Fig. 7. **Comparison of apoptosis-inducing activities among four types of cermides.** (A) Apoptotic cells were detected as exposure of phosphatidylserine on the cell surface by flow cytometry. The representative results of HL60 cells, after the treatment with or without 0.3 μM of Cer 3 for 16 h, were shown. The percentages of early (annexin V positive and 7-AAD negative) and late (annexin V positive and 7-AAD positive) apoptotic cells were increased from 2.1% to 6.8% and from 2.2% to 20.4%, respectively, in the treated cells (right panel), compared with those in untreated cells (left panel). (B) Western blot analysis for PARP cleaved by caspase-3. Bands were visualized with ECL system. HL60 cells were treated with or without 0.2 μM of Cer 1, Cer 2, Cer 3 and Cer 4 for 16 h. Intact PARP at 115 kDa was detected in all samples, whereas cleaved PARP at 85 KDa was detected in samples treated with Cer 2 and Cer 3. (C) Caspase-3 activities of HL60 cells induced by 16-h-incubation with 0.2 μM of ceramides. The values are means ± SD (n = 3). Significant differences are shown as $^{*}P < 0.05$, $^{**}P < 0.005$ and $^{***}P < 0.001$.

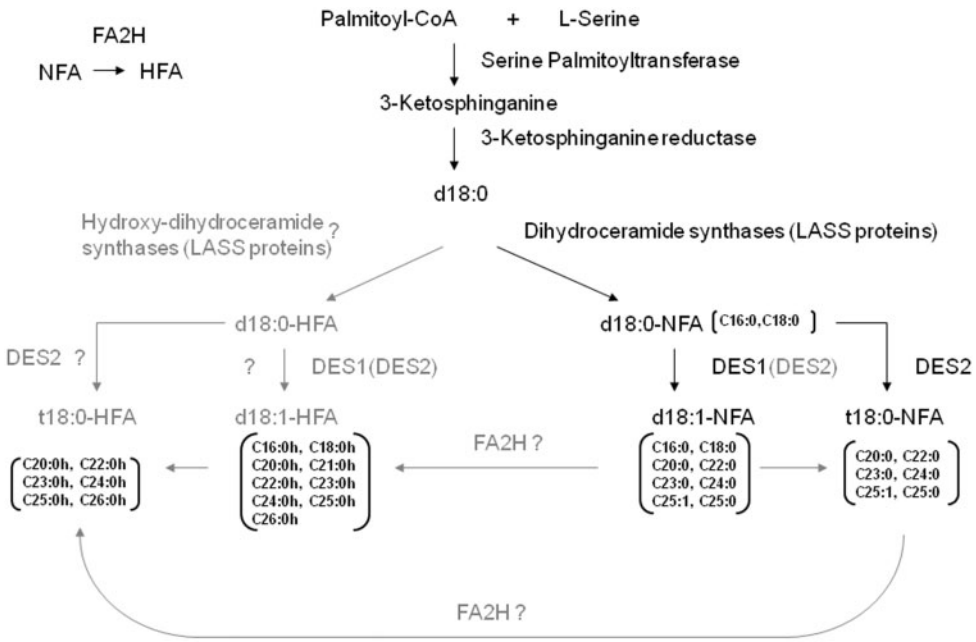

Fig. 8. **Proposed *de novo* synthetic pathway for major ceramide species possessing OD-LCBs.** Identified pathways and proposed pathways are shown in black and grey, respectively.

Table 3. **Combination of long-chain bases with fatty acids.**

	d16:1	t16:0	d17:1	t17:0	d18:1	d18:0	t18:0	d19:1	t19:0	d20:1	t20:0
NFA											
(C16:0)	–	–	–	–	+	+	+	–	–	–	–
(C18:0)	–	–	–	–	+	+	+	–	–	–	+
(C20:0)	–	+	–	–	+	–	+	–	–	–	–
(C22:0)	–	–	–	–	+	–	+	–	–	–	+
(C23:0)	–	–	–	–	+	–	+	–	–	–	+
(C24:0)	–	–	–	–	+	–	+	–	+	–	+
(C25:1)	–	–	–	–	+	–	+	–	–	–	–
(C25:0)	–	–	–	–	+	–	+	–	–	–	–
(C26:0)	–	–	–	–	+	–	+	–	–	–	–
HFA											
(C16:0h)	–	–	–	–	+	–	+	–	–	–	–
(C18:0h)	–	–	–	–	+	–	+	–	–	–	–
(C19:0h)	–	–	–	–	+	–	–	–	–	–	+
(C20:0h)	+	+	+	–	+	–	+	–	–	–	+
(C21:0h)	+	–	–	–	+	–	+	–	–	–	–
(C22:0h)	+	–	+	+	+	–	+	–	+	+	+
(C23:0h)	+	+	+	–	+	–	+	–	+	+	+
(C24:0h)	–	–	+	+	+	–	+	+	+	+	+
(C25:0h)	–	–	–	–	+	–	+	–	–	–	–
(C26:0h)	–	–	–	–	+	–	+	–	–	–	–

REFERENCES

1. Hirabayashi, Y. Igarashi Y. Merrill A. H. Jr. (2006) Sphingolipids synthesis, transport and cellular signaling in Sphingolipid Biology (Hirabayashi Y. Igarashi Y. Merrill A. H. Jr. eds.) pp. 3–22, Springer, Tokyo
2. Hill, J.R. and Wertz, P.W. (2003) Molecular models of the intercellular lipid lamellae from epidermal stratum corneum. *Biochim. Biophys. Acta* **1616**, 121–126
3. Kolesnick, R.N., Goni, F.M., and Alonso, A. (2000) Compartmentalization of ceramide signaling: physical foundations and biological effects. *J. Cell. Physiol.* **184**, 285–300
4. Merrill, A.H. Jr. (2002) De novo sphingolipid biosynthesis: a necessary, but dangerous, pathway. *J. Biol. Chem.* **277**, 25843–25846
5. Ogretmen, B. and Hannun, Y.A. (2004) Biologically active sphingolipids in cancer pathogenesis and treatment. *Nat. Rev. Cancer.* **4**, 604–616
6. Taha, T.A., Mullen, T.D., and Obeid, M.L. (2006) A house divided: ceramide, sphingosine, and sphingosine-1-phosphate in programmed cell death. *Biochim. Biophys. Acta* **1758**, 2027–2036
7. Gu, M., Kerwin, J.L., Watts, J.D., and Aebersold, R. (1997) Ceramide profiling of complex lipid mixtures by electrospray ionization mass spectrometry. *Anal. Biochem.* **244**, 347–356
8. Liebisch, G., Drobnik, W., Reil, M., Trumbach, B., Arnecke, R., Olgemoller, B., Roscher, A., and Schmitz, G. (1999) Quantitative measurement of different ceramide species from crude cellular extracts by electrospray ionization tandem mass spectrometry (ESI-MS/MS). *J. Lipid Res.* **40**, 1539–1546
9. Hsu, F.F. and Turk, J. (2002) Characterization of ceramides by low energy collisional-activated dissociation tandem mass spectrometry with negative-ion electrospray ionization. *J. Am. Soc. Mass Spectrom.* **13**, 558–570
10. Hsu, F.F., Turk, J., Stewart, M.E., and Downing, D.T. (2002) Structural studies on ceramides as lithiated adducts by low energy collisional-activated dissociation tandem mass spectrometry with electrospray ionization. *J. Am. Soc. Mass Spectrom.* **13**, 680–695
11. Merill, A.H. Jr. Sullards, M.C., Allegood, J.C., Kelly, S., and Wang, E. (2005) Sphingolipidomics: high-throughput, structure-specific, and quantitative analysis of sphingolipids by liquid chromatography tandem mass spectrometry. *Methods* **36**, 207–224
12. Valsecchi, M., Mauri, L., Casellato, R., Prioni, S., Loberto, N., Prinetti, A., Chigorno, V., and Sonnino, S. (2007) Ceramide and sphingomyelin species of fibroblasts and neurons in culture. *J. Lipid Res.* **48**, 417–424
13. Masukawa, Y., Tsujimura, H., and Narita, H. (2006) Liquid chromatography-mass spectrometry for comprehensive profiling of ceramide molecules in human hair. *J. Lipid Res.* **47**, 1559–1571
14. Karlsson, K.A. (1970) On the chemistry and occurrence of sphingolipid long-chain bases. *Chem. Phys. Lipids.* **5**, 6–43
15. Hara, A. and Taketomi, T. (1975) Long chain base and fatty acid compositions of equine kidney sphingolipids. *J. Biochem.* **78**, 527–536
16. Kyogashima, M., Tamiya-Koizumi, K., Ehara, T., Li, G., Hu, R., Hara, A., Aoyama, T., and Kannagi, R. (2006) Rapid demonstration of diversity of sulfatide molecular species from biological materials by MALDI-TOF MS. *Glycobiology* **16**, 719–728
17. Matsuda, J., Kido, M., Tadano-Aritomi, K., Ishizuka, I., Tominaga, K., Toida, K., Takeda, E., Suzuki, K., and Kuroda, Y. (2004) Mutation in saposin D domain of sphingolipid activator protein gene causes urinary system defects and cerebellar Purkinje cell degeneration with accumulation of hydroxy fatty acid-containing ceramide in mouse. *Hum. Mol. Genet.* **13**, 2709–2723
18. Ji, L., Zhang, G., Uematsu, S., Akahori, Y., and Hirabayashi, Y. (1995) Induction of apoptotic DNA fragmentation and cell death by natural ceramide. *FEBS Lett.* **358**, 211–214
19. van Engeland, M., Kuijpers, H.J., Ramaekers, F.C., Reutelingsperger, C.P., and Schutte, B. (1997) Plasma membrane alterations and cytoskeletal changes in apoptosis. *Exp. Cell Res.* **235**, 421–430
20. Lazebnik, Y.A., Kaufmann, S.H., Desnoyers, S., Poirier, G.G., and Earnshaw, W.C. (1994) Cleavage of poly (ADP-ribose) polymerase by a proteinase with properties like ICE. *Nature* **371**, 346–347
21. Hanada, K. (2003) Serine palmitoyltransferase, a key enzyme of sphingolipid metabolism. *Biochim. Biophys. Acta* **1632**, 16–30

22. Hornemann, T., Wei, Y., and von Eckardstein, A. (2007) Is the mammalian serine-palmitoyltransferase a high molecular weight complex? *Biochem. J.* **405**, 157–164
23. Williams, R.D., Wang, E., and Merrill, A.H. Jr. (1984) Enzymology of long-chain base synthesis by liver: characterization of serine palmitoyltransferase in rat liver microsomes. *Arch. Biochem. Biophys.* **228**, 282–291
24. Merrill, A.H. Jr, Wang, E., and Mullins, R.E. (1988) Kinetics of long-chain (sphingoid) base biosynthesis in intact LM cells: effects of varying the extracellular concentrations of serine and fatty acid precursors of this pathway. *Biochemistry* **27**, 340–345
25. Michel, C., van Echten-Deckert, G., Rother, J., Sandhoff, K., Wang, E, and Merrill, A.H. Jr. (1997) Characterization of ceramide synthesis. A dihydroceramide desaturase introduces the 4,5-trans-double bond of sphingosine at the level of dihydroceramide. *J. Biol. Chem.* **272**, 22432–22437
26. Venkataraman, K., Riebeling, C., Bodennec, J., Riezman, H., Allegood, J.C., Sullards, M.C., Merrill, A.H. Jr, and Futerman, A.H. (2002) Upstream of growth and differentiation factor 1 (uog1), a mammalian homolog of the yeast longevity assurance gene 1 (LAG1), regulates N-stearoyl-sphinganine (C18-(dihydro)ceramide) synthesis in a fumonisin B1-independent manner in mammalian cells. *J. Biol. Chem.* **277**, 35642–35649
27. Lahiri, S. and Futerman, A.H. (2005) LASS5 is a bona fide dihydroceramide synthase that selectively utilizes palmitoyl-CoA as acyl donor. *J. Biol. Chem.* **280**, 33735–33738
28. Riebeling, C., Allegood, J.C., Wang, E., Merrill, A.H. Jr., and Futerman, A.H. (2003) Two mammalian longevity assurance gene (LAG1) family members, trh1 and trh4, regulate dihydroceramide synthesis using different fatty acyl-CoA donors. *J. Biol. Chem.* **278**, 43452–43459
29. Mizutani, Y., Kihara, A., and Igarashi, Y. (2005) Lass6 and its related family members regulate synthesis of specific ceramides. *Biochem. J.* **390**, 263–271
30. Ternes, P., Franke, S., Zahringer, U., Sperling, P., and Heinz, E. (2002) Identification and characterization of a sphingolipid delta 4-desaturase family. *J. Biol. Chem.* **277**, 25512–25518
31. Omae, F., Miyazaki, M., Enomoto, A., and Suzuki, A. (2004) Identification of an essential sequence for dihydroceramide C-4 hydroxylase activity of mouse DES2. *FEBS Lett.* **576**, 63–67
32. Alderson, N.L., Rembiesa, B.M., Walla, M.D., Bielawska, A., Bielawski, J., and Hama, H. (2004) The human FA2H gene encodes a fatty acid 2-hydroxylase. *J. Biol. Chem.* **279**, 48562–48568
33. Alderson, N.L., Maldonado, E.N., Kern, M.J., Bhat, N.R., and Hama, H. (2006) FA2H-dependent fatty acid 2-hydroxylation in postnatal mouse brain. *J. Lipid Res.* **47**, 2772–2780
34. Eckhardt, M., Yaghootfam, A., Fewou, S.N., Zoller, I., and Gieselmann, V. (2005) A mammalian fatty acid hydroxylase responsible for the formation of alpha-hydroxylated galactosylceramide in myelin. *Biochem. J.* **388**, 245–254
35. Enomoto, A., Omae, F., Miyazaki, M., Kozutsumi, Y., Yubisui, T., and Suzuki, A. (2006) Dihydroceramide : sphinganine C-4-hydroxylation requires DES2 hydroxylase and the membrane form of cytochrome b5. *Biochem. J.* **397**, 289–295
36. Omae, F., Miyazaki, M., Enomoto, A., Suzuki, M., Suzuki, Y., and Suzuki, A. (2004) DES2 protein is responsible for phytoceramide biosynthesis in the mouse small intestine. *Biochem. J.* **379**, 687–695
37. Mizutani, Y., Kihara, A., and Igarashi, Y. (2004) Identification of the human sphingolipid C4-hydroxylase, hDES2, and its up-regulation during keratinocyte differentiation. *FEBS Lett.* **563**, 93–97
38. Dickson, R. and Lester, R. (2006) Current perspectives on saccharomyces cerevisiae sphingolipids in *Sphingolipid Biology* (Hirabayashi, Y., Igarashi, Y., and Merril, A.H. Jr, eds.) pp. 141–150, Springer, Tokyo
39. Stallberg-Staenhagen, S. and Svennerholm, L. (1965) Fatty acid composition of human brain sphingomyelins: normal variation with age and change during myelin disorders. *J. Lipid Res.* **6**, 146–155
40. Lee, J.S., Min, D.S., Park, C., Park, C.S., and Cho, N.J. (2001) Phytosphingosine and C2-phytoceramide induce cell death and inhibit carbachol-stimulated phospholipase D activation in Chinese hamster ovary cells expressing the Caenorhabditis elegans muscarinic acetylcholine receptor. *FEBS Lett.* **499**, 82–86
41. Hwang, O., Kim, G., Jang, Y.J., Kim, S.W., Choi, G., Choi, H.J., Jeon, S.Y., Lee, D.G., and Lee, J.D. (2001) Synthetic phytoceramides induce apoptosis with higher potency than ceramides. *Mol. Pharmacol.* **59**, 1249–1255
42. Graf, K., Baltes, H., Ahrens, H., Helm, CA., and Husted, C.A. (2002) Structure of hydroxylated galactocerebrosides from myelin at the air-water interface. *Biophys. J.* **82**, 896–907
43. Carter, H.E. and Hirschberg, C.B. (1968) Phytosphingosines and branched sphingosines in kidney. *Biochemistry* **7**, 2296–2300
44. Kitano, Y., Iwamori, Y., Kiguchi, K., DiGiovanni, J., Takahashi, T., Kasama, K., Niwa, T., Harii, K., and Iwamori, M. (1996) Selective reduction in alpha-hydroxypalmitic acid-containing sphingomyelin and concurrent increase in hydroxylated ceramides in murine skin tumors induced by an initiation-promotion regimen. *Jpn. J. Cancer Res.* **87**, 437–441
45. Karlsson, A.A., Michelsen, P., and Odham, G. (1998) Molecular species of sphingomyelin: determination by high-performance liquid chromatography/mass spectrometry with electrospray and high-performance liquid chromatography/tandem mass spectrometry with atmospheric pressure chemical ionization. *J. Mass Spectrom.* **33**, 1192–1198
46. Ledeen, R.W. and Wu, G. (2006) Sphingolipids of the nucleus and their role in nuclear signaling. *Biochim. Biophys. Acta* **1761**, 588–598
47. Ardail, D., Popa, I., Alcantara, K., Pons, A., Zanetta, J.P., Louisot, P., Thomas, L., and Portoukalian, J. (2001) Occurrence of ceramides and neutral glycolipids with unusual long-chain base composition in purified rat liver mitochondria. *FEBS Lett.* **488**, 160–164
48. Siskind, L.J. (2005) Mitochondrial ceramide and the induction of apoptosis. *J. Bioenerg. Biomembr.* **37**, 143–153